Hindawi
Advances in Materials Science and Engineering
Volume 2021, Article ID 9930929, 15 pages
https://doi.org/10.1155/2021/9930929

Research Article

Analytical and Numerical Study of the Ground Pressure of the Work Face Crossing the Fault

Yanan Gao,[1,2,3] Yudong Zhang ,[1,2] Donghao Lan,[1,2] and Feng Gao[1,2]

[1]*State Key Laboratory for Geomechanics and Underground Engineering, China University of Mining and Technology, Xuzhou, Jiangsu 221116, China*
[2]*School of Mechanics and Civil Engineering, China University of Mining and Technology, Xuzhou, Jiangsu 221116, China*
[3]*Key Laboratory of Deep Earth Science and Engineering, Sichuan University, Chengdu, Sichuan 610025, China*

Correspondence should be addressed to Yudong Zhang; 1065686075@qq.com

Received 30 March 2021; Accepted 11 May 2021; Published 20 May 2021

Academic Editor: Xianjie Hao

The excavation of coal mine often encounters the fault problem. In this paper, the analytical study of the pressure of the fault that the work face may cross is carried out. The evolution of the stress and moment of the fault is investigated. Afterwards, a numerical study is performed. The stress and displacement of the rock mass near the work face and the fault are calculated under each situation (the initial fracture and periodical fracture of the immediate roof, the forward direction fault, and the reverse direction fault), and the changes in the contact pressure and stress near the fault during the excavation are analyzed. The effect of searching tunnel on the mining pressure is also studied. The calculation results indicate that although the searching-tunnel can decrease the stress at the roof of the fault (reverse direction fault), it may increase the stress at other positions. It can therefore be concluded that, for the forward direction fault, the effect of the searching tunnel to decrease the contact pressure and dissipate the energy is limited; on the contrary, it will aggravate the fragmentation degree and make the support more difficult, while, for the reverse direction fault, the excavation of searching tunnel can not only provide a better understanding of the characters of the fault but also have a positive effect on the ground control.

1. Introduction

Coal is one of the most important energy sources in the world and one of the main energy sources used by human beings since the eighteenth century and is known as the "real staple food" in industry. China is the largest country in coal consumption in the world, and coal accounts for more than 55% of the total primary energy consumption. Although the proportion of clean energy sources, such as hydropower, wind power, and nuclear power, continues to increase, the dominant position of coal will be difficult to change in a short period of time. The coal-based energy structure supports the rapid development of Chinese economy. In 2021, the total consumption of coal will stabilize at about 41.8 billion tons [1–4].

Ground pressure which is induced by the mining disturbance is a major safety problem during coal mining. With the continuous improvement of coal mining equipment, technology, and the improvement of safety supervision system, coal mine accidents have been effectively prevented and controlled, and the number of safety accidents has decreased year by year [5, 6]. However, the roof disaster can be induced by many causes, and such disaster is easy to burst and difficult to prevent and control. It is still an important factor effecting the coal mine safety production [7–9]. The analysis of the characteristics of roof disaster and the study of the law of roof activities are the key to the prevention and control of surrounding rock disasters [10, 11]. Ground pressure can be generally classified as the initial pressure and the periodic pressure. The initial pressure is dramatic, and it may cause a step-like subsidence of the roof and serious damage to the supporting. Compared with the initial pressure, the periodic pressure is relatively moderate and the ground pressure may increase periodically [12]. According

to the different actual situation of coal seam, the mine pressure produced by it is also different.

At present, many studies have been carried out to exploration the problem of ground pressure. Yan et al. adopted SOS microseismic monitoring system, numerical simulation to study the microseismic law of fully-mechanized work face with a fault [13]. Shi et al. analyzed the special mine pressure law and put forward the mechanical model of special coal pillar [14]. Cai et al. proposed a method of characterizing rock mass damage near excavations based on microseismic event monitoring. And a damage numerical model, which takes the microseismic data as input to determine the damage state described by fracture density, was presented. It was found that when damage related softening based on microseismic data was considered, the predicted displacements of the rock mass were in good agreement with extensometer measurements [15]. Suchowerska et al. identified the relative magnitude of horizontal stress change below a series of parallel longwall panels as a consequence of multiseam mining; the key findings of this research are that the maximum horizontal stress would approximately have a 10% of the original in situ horizontal stress for the case of isotropic rock strata [16]. Jiang et al. provided treatment measures, such as design of the position of the longwall panel, rational arrangement of roadways, stress prereleasing, and enhancement of monitoring [17]. Meanwhile, there are many studies about the mining induced deformation and failure behaviors of the rock. Based on the physical model, Lou et al. pointed out that the tensile principal stress is inversely arched before the first breaking, and the breaking line forms an obtuse angle with the advancing direction of the panel during the periodic breaking [18]. With the mining/excavation disturbance background, Hao et al. studied the crack initiation and propagation under the static-dynamic loading conditions, the evolution of the strength, crack properties such as direction and type are studied with the loading rate and the proportion of the static and dynamic loads, and the anisotropy effected are detailed analyzed [19, 20]. Zhang et al. proposed a comparison study of the rock fracture network evolution under the three different stress paths of mining disturbance (top-coal caving mining—TCM, nonpillar mining—NM, and protective coal-seam mining—PCM), and they pointed out that the degree of fragmentation/fracture network complexity of the rock increases by PCM, NM, and TCM conditions [21]. In addition, the mining depth is also a key factor for the properties of the rock; the deformation, damage behavior, and the energy transformation and transition mechanism are significantly different for different depth [22].

A fault that exists in front of a work face will affect the ground pressure greatly. It is necessary to investigate the direction of the work face excavation. Based on a coal mine of Yanzhou area, this paper presents a comparative study on the law of ground pressure behavior of the working face of under the forward direction fault and the reverse direction fault. Based on the theory of material mechanics, the mechanical model of the roof is established. The initial breaking distance and maximum tensile stress of the roof for both of the forward direction fault and reverse direction fault are studied. The simulation of the working face crossing through the fault is carried out. The law of ground pressure behavior of working face through the forward direction fault and reverse direction fault is investigated via a numerical method.

The influence of the searching tunnel on the pressure behavior of working face passing through fault is analyzed. The relevant models are established to study whether the contact stress at the fault, displacement, and stress of roof are improved if the searching tunnel is excavated. Here, the concept of the searching should be stressed. It is different from exploration roadway [23] which is used to find out the geological conditions.

2. The Analysis of Mechanics Model of Work Face Crossing the Fault

The mechanical model of the work face with the fault is shown in Figure 1. The left and right ends of the model are fixed, and a uniformly distributed force q is applied immediately on the roof. The overburden pressure is simplified as q. The faults in this paper are different from the normal faults mentioned in coal geology. After the formation of a fault, the hanging wall is relatively down; the floor that is relatively higher than the fault is called normal fault [24]. Currently, an inclined fault occurs on the roof of the coal seam (Figure 1). When the mining direction and the fault dip angle are less than 90°, the fault is defined as the forward direction fault; when the mining direction and fault dip angle are greater than 90°, the fault is defined as the reverse direction fault.

2.1. Forward Direction Fault [25, 26]. The schematic diagram of the above fault structure is simplified as a cantilever beam model. The left end of the cantilever beam is the fixed end, and the right end is the free end (Figure 2). The upside of the beam is subjected to the uniform load p_1, and the underside is subjected to the uniform load p_2. The action length of p_2 is a, the right end is subjected to the shear force F. The length of the beam is l, the height of the beam section is h, and the breadth of section is b. According to the cantilever beam and simply supported beam model, the stress of the immediate roof in the initial and periodic fracture can be deduced.

2.1.1. Initial Facture. When $0 \le x \le l - a$, the bending moment at x can be written as

$$M(x) = F(l-x) + \frac{P_1}{2}(l-x)^2 - P_2 a\left(l - x - \frac{a}{2}\right), \quad (1)$$

$$M = \frac{1}{6}bh^2\sigma_b, \quad (2)$$

$$\sigma(x) = \frac{6F(l-x)}{bh^2} + \frac{3P_1(l-x)^2}{bh^2} - \frac{6P_2(l-x-(a/2))}{bh^2}, \quad (3)$$

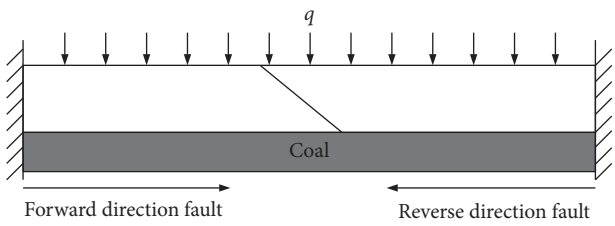

Figure 1: The mechanical model of the forward direction fault and the reverse direction fault.

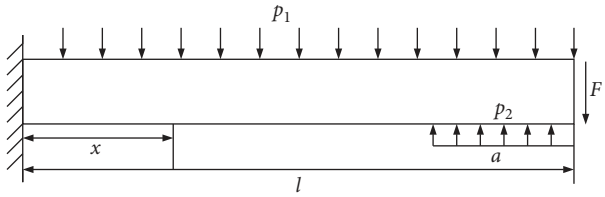

Figure 2: The mechanics model of forward direction fault (the initial fracture).

If $l = 50\,\text{m}$, $a = 20\,\text{m}$, $h = 1\,\text{m}$, $P_1 = 2000\,\text{N/m}$, $P_2 = 4500\,\text{N/m}$, $F = 4000\,\text{N}$, the evolution of the bending moment and the stress of the beam is shown in Figures 3 and 4. Both the maximum value of the moment and the stress occur about 7.5 m to the left end.

Figure 3 is the variation of bending moment with the assumption that fracture position is in the range of $0 \le x \le l - a$. Figure 4 is the variation of bending stress with the assumption that fracture position is in the range of $0 \le x \le l - a$.

The initial facture distance is calculated as

$$x = \frac{F + P_1 l - P_2 a}{P_1} \pm \sqrt{\left(\frac{F - P_2 a}{P_1}\right)^2 + \left(\frac{bh^2\sigma_b - 3P_2 a^2}{3P_1}\right)}, \tag{4}$$

The cantilever beam produces the maximum bending moment at x.

When $l - a < x \le l$, the bend moment $M(x)$ can be written as

$$M(x) = F(l - x) + P_1\frac{(l - x)^2}{2} - P_2\frac{(l - x)^2}{2}, \tag{5}$$

$$\sigma(x) = \frac{6F(l - x)}{bh^2} + \frac{3P_1(l - x)^2}{bh^2} - \frac{3P_2(l - x)^2}{bh^2}, \tag{6}$$

The evolution of the bending moment and the stress of the beam is shown in Figures 5 and 6. The maximum stress is produced on the cantilever beam during $0 \le x \le l - a$. Therefore, the section in which the cantilever beam is broken is $0 \le x \le l - a$.

Figure 5 is the variation of bending moment with the assumption that fracture position is in the range of $l - a < x \le l$. Figure 6 is the variation of bending stress with the assumption that fracture position is in the range of $l - a < x \le l$.

Based on the results of stress and moment shown in Figures 3–6, the maximum value of the moment and the stress are at $x = 7.5\,\text{m}$, which is prone to instability and failure.

2.1.2. Periodical Facture. Periodical facture can be simplified as a simply supported beam mode (Figure 7). To set the balance distance of rotation as l_1, the moment equilibrium equation can be written as

$$Fl_1 + P_1\frac{l_1^2}{2} + P_2 a\left(l_1 - a + \frac{a}{2}\right) = 0. \tag{7}$$

Thus, l_1 can be expressed as

$$l_1 = \sqrt{\frac{P_2}{P_1}a^2 + \frac{(P_2 a + F)^2}{P_1^2}} - \frac{P_2 a + F}{P_1}. \tag{8}$$

The periodical facture distance expression can be obtained by replacing l in x expression with l_1.

2.1.3. Mechanics Analysis of the Fault. The fault is shown in Figure 8. It is assumed that the upside of the working face is subjected to uniform load P_1, the underside is subjected to uniform load P_2 with length a, the angle θ between fault plane and vertical direction is narrow, and the vertical direction load is P_3. When calculating the stress at the fault, it can be regarded as a problem of variable cross section beam.

$$h(\xi) = \frac{l' - \xi}{\tan\theta}, \tag{9}$$

$$M(\xi) = \frac{1}{2}(P_2 - P_3)(l'\xi)^2, \tag{10}$$

$$\begin{aligned}\sigma(\xi) &= \frac{M(\xi)}{W_Z(\xi)} \\ &= \frac{(1/2)(P_2 - P_3)(l' - \xi)^2}{((l' - \xi)/\tan\theta)^2/6} \\ &= 3(P_2 - P_3)\cot^2\theta.\end{aligned} \tag{11}$$

Therefore, the stress in the fault is a constant.

In this section, the theory of materials mechanics is employed to present the equations of the stresses and moments. The basic equations and assumptions can be found in any books or references of material mechanics. Equations (1)–(10) are also listed in the previous work of our group [25, 26]. The parameter calculation and the judgement of the position of initial fracture based on the plots of bending moment and bending stress is discussed in this paper.

2.2. Reverse Direction Fault. Similar to the forward direction fault, the reverse direction fault is also simplified to a cantilever beam model. The corresponding loads are applied as in Figure 9.

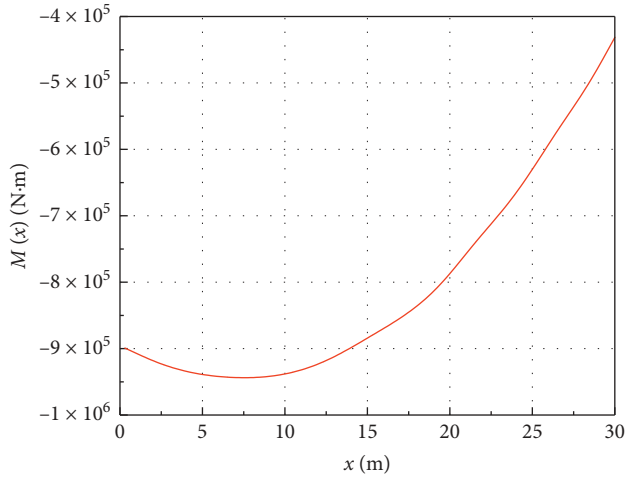

Figure 3: The variation of bending moment (I).

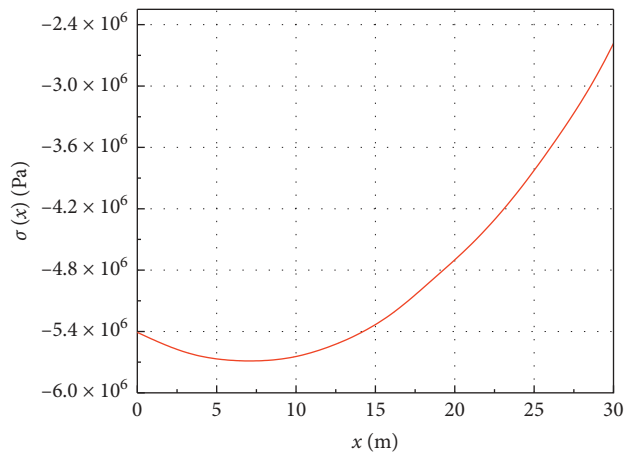

Figure 4: The variation of bending stress (I).

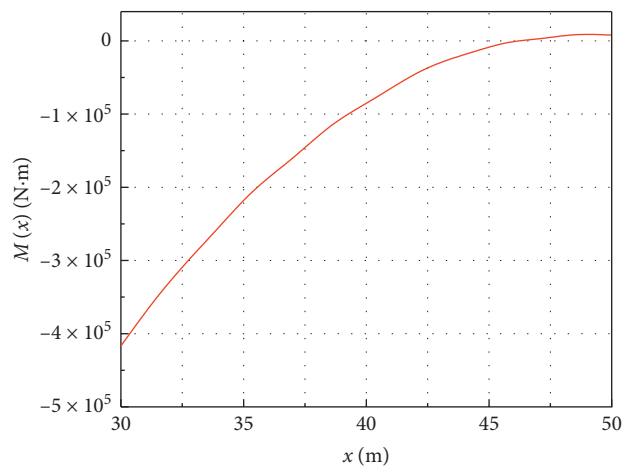

Figure 5: The variation of bending moment (II).

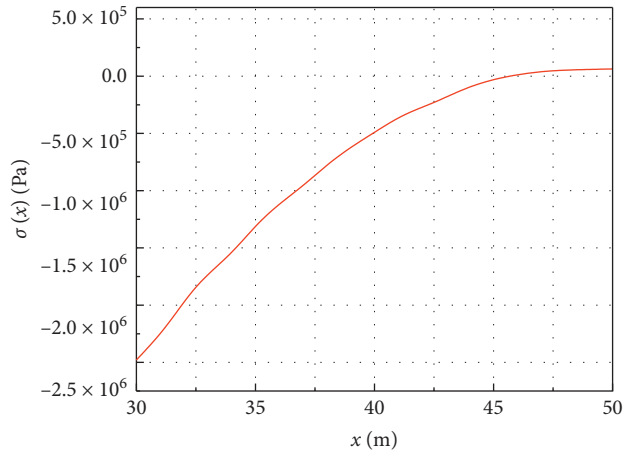

Figure 6: The variation of bending stress (II).

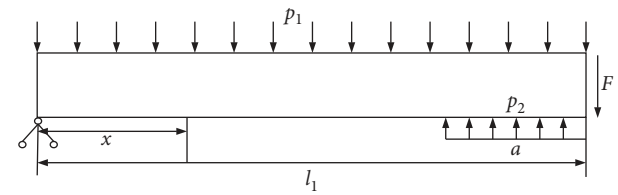

Figure 7: The mechanical model of forward direction fault (the periodical fracture).

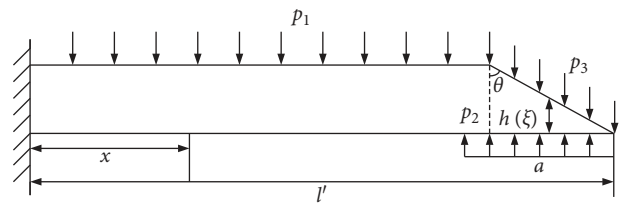

Figure 8: The mechanics model of the forward direction fault.

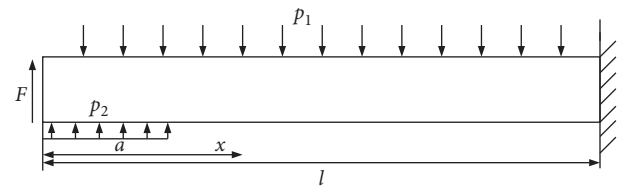

Figure 9: The mechanics model of reverse direction fault (the initial fracture).

2.2.1. Initial Facture. When $0 \le x \le l - a$, the bending moment at x can be written as

$$M(x) = P_1\frac{x^2}{2} - P_2\frac{x^2}{2} - Fx,$$
$$\sigma(x) = \frac{3P_1x^2}{bh^2} - \frac{3P_2x^2}{bh^2} - \frac{6Fx}{bh^2}. \quad (12)$$

If $l = 50\,\text{m}$, $a = 20\,\text{m}$, $h = 1\,\text{m}$, $P_1 = 2000\,\text{N/m}$, $P_2 = 4500\,\text{N/m}$, $F = 4000\,\text{N}$, the evolution of the bending moment and the stress of the beam is shown in Figures 10 and 11. Figure 10 is the variation of bending moment with the assumption that fracture position is in the range of $0 \le x \le l - a$. Figure 11 is the variation of bending stress with the assumption that fracture position is in the range of $0 \le x \le l - a$. Both the maximum values of the moment and the stress occur about 20 m to the left end.

Let $M = M_{\max}$; the initial facture distance can be obtained:

$$x = \frac{F}{P_1 - P_2} + \sqrt{\left(\frac{F}{P_1 - P_2}\right)^2 + \frac{bh^2\sigma_b}{3(P_1 - P_2)}}. \tag{13}$$

When $a < x \le l$,

$$M(x) = P_1\frac{x^2}{2} - P_2 a\left(x - a + \frac{a}{2}\right) - Fx,$$
$$\sigma(x) = \frac{3P_1x^2}{bh^2} - \frac{6P_2a(x - a + (a/2))}{bh^2} - \frac{6Fx}{bh^2}. \tag{14}$$

Figure 12 is the variation of bending moment with the assumption that fracture position is in the range of $a < x \le l$. Figure 13 is the variation of bending stress with the assumption that fracture position is in the range of$a < x \le l$.

The evolution of the bending moment and the stress of the beam is shown in Figures 12 and 13. The maximum stress is produced on the cantilever beam during $a < x \le l$. Therefore, the fracture position of the cantilever beam should be in the range of $a < x \le l$.

Based on the results of stress and moment shown in Figures 10–13, the maximum values of the moment and the stress are at the position of 50 m to the left end. Therefore, such position is prone to instability and failure.

Let $M = M_{\max}$:

$$x = \frac{P_2a + F}{P_1} + \sqrt{\left(\frac{P_2a + F}{P_1}\right)^2 - \frac{3P_2a^2 - bh^2\sigma_b}{3P_1}}. \tag{15}$$

Thus, the bending moment at the coal wall is as follows:

$$M' = P_1\frac{l^2}{2} - P_2a\left(l - \frac{a}{2}\right) - Fl. \tag{16}$$

The tensile stress at the coal wall is obtained as follows:

$$\sigma'_{\max} \frac{3P_1l^2}{bh^2} - \frac{6P_2a(l - (a/2))}{bh^2} - \frac{6Fl}{bh^2}. \tag{17}$$

2.2.2. Periodical Facture. Similarly, the periodical fracture of the roof can be simplified to a simply supported beam mode (Figure 14).

To assume that, the rotation balance distance is l_1, and the moment at the support can be written as

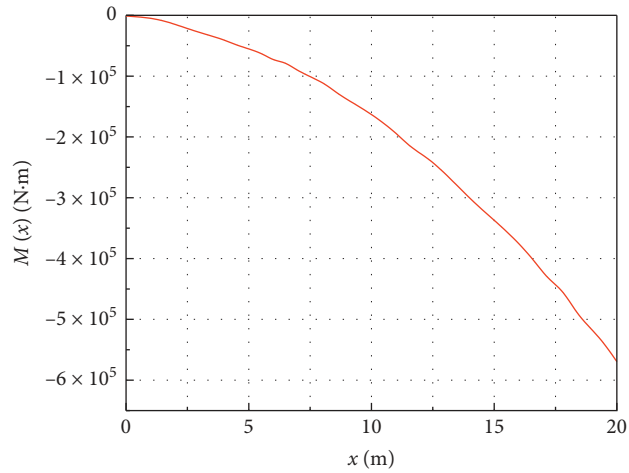

Figure 10: The variation of bending moment (III).

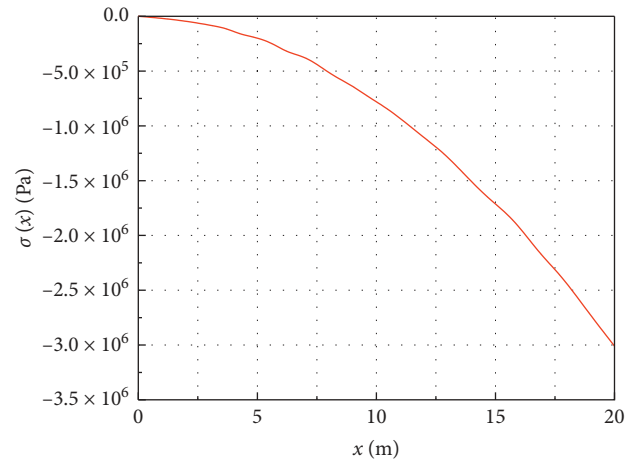

Figure 11: The variation of bending stress (III).

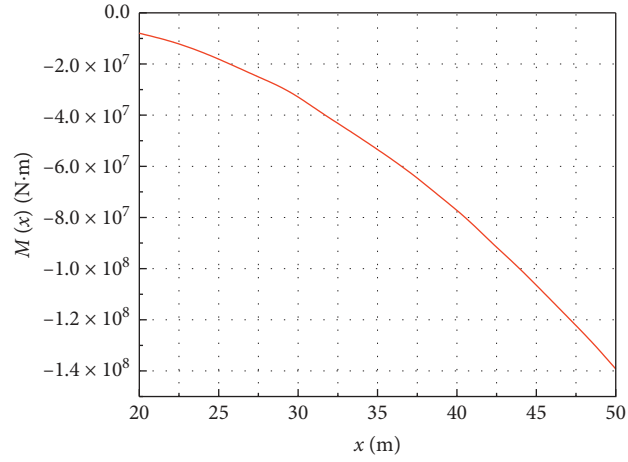

Figure 12: The variation of bending moment (IV).

$$P_1\frac{l_1^2}{2} - P_2a\left(l_1^2 - \frac{a}{2}\right) - Fl_1^2 = 0. \tag{18}$$

It can be obtained that

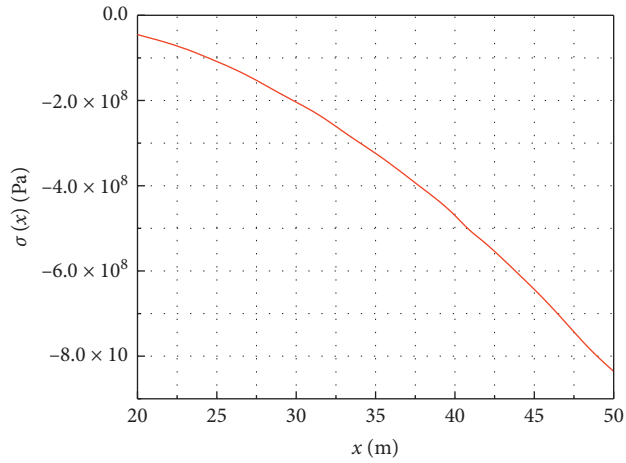

Figure 13: The variation of bending stress (IV).

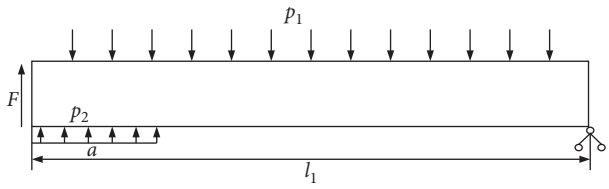

Figure 14: The mechanical model of reverse direction fault (the periodical fracture).

$$l_1 = \frac{P_2 a + F}{P_1} - \sqrt{\left(\frac{P_2 a + F}{P_1}\right)^2 - \frac{P_2}{P_1} a^2}. \tag{19}$$

2.2.3. Mechanics Analysis of the Fault. The fault is shown in Figure 15.

$$\begin{aligned} h(\xi) &= \frac{\xi}{\tan\theta}, \\ M(\xi) &= \frac{1}{2}(P_3 - P_1)\xi^2, \\ \sigma(\xi) &= \frac{M(\xi)}{W_Z(\xi)} \\ &= \frac{(1/2)(P_3 - P_1)\xi^2}{(\xi/\tan\theta)^2/6} \\ &= 3(P_3 - P_1)\cot^2\theta. \end{aligned} \tag{20}$$

Therefore, the stress in the fault is a constant. And the distribution of the stress on the reverse direction fault is the same as that on the forward direction fault.

3. Numerical Analysis of Mining Pressure

Three situations are the work face far from the fault, near it, and under it, mainly simulated in the exploitation process. For the actual fault situation, we can solve the problem in two sections, forward and reverse fault. For the different fault cases, the effect of exploitation to stratum is different, although the mechanics model is the same. For the same fault case, the mechanics behaviors of the roof or the fault are different during the different fracture process. Therefore, we may subdivide the problem as initial fracture and the periodical fracture in the numerical analysis.

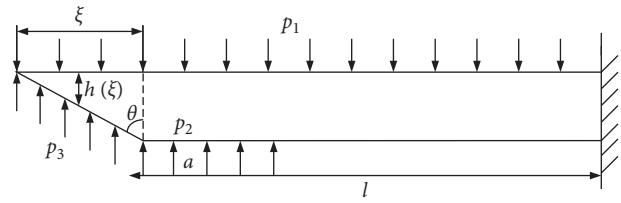

Figure 15: The mechanics model of the reverse direction fault.

3.1. Establishment of Simulated Mechanics Model. According to the actual situation, the four models are established. Every model can be modeled with the searching tunnel or without it.

For the situation with the searching tunnel or not, the same model can be used and the elements of the tunnel are "killed" when the tunnel is needed. The exploitation process for every model is simulated; thus the exact exploitation process and a result close to the actual situation can be obtained. Material parameters are shown in Table 1. As shown in Figures 16 and 17, the "support" is used to model the hydraulic support which is used in mined out area. The sketch of the four models is shown in Figures 16–19.

The length of model is 150 meters; the angle of fault is 60°. The simulation is carried out by using the FEM software ANSYS.

3.2. Result and Analysis of Simulated Calculation. The results of simulation are shown in Figures 20–25 and Table 2. According to Figures 20–25, the roof above the mined-out area is the most dangerous area; the stresses and deformations at the site are significant. For the forward direction fault case, the working face is under fault; the stress above mined-out area redistributes continuously with the increase of the mined-out area. For the reverse direction fault case, the fault is far from the mined-out area and the stress is less affected by mined-out area; the stress in reverse direction fault is mainly in situ stress. Therefore, the difference of contact pressure between forward direction fault and reverse direction is great. Figures 20(a), 21(a), and 22(a) can also been found in [25] or [26]. Meanwhile, the nephograms of contact pressure in Figures 20–25 are the initial fracture situation. For the periodical fracture situation, the nephograms are not presented in this paper because of space; the related nephograms can be found in [25].

As shown in Figures 26 and 27, the contact pressure of reverse fault is generally more than that of forward fault. When the initial fracture occurs, the pressure of the

Table 1: Material parameters.

Material/property	E (Pa)	μ	Height (m)
Main roof	3×10^{10}	0.25	25
Immediate roof	4×10^{10}	0.3	5
Coal bed	1.6×10^{10}	0.15	4.5
Floor	3.5×10^{10}	0.3	5
Support	2×10^{11}	0.3	—

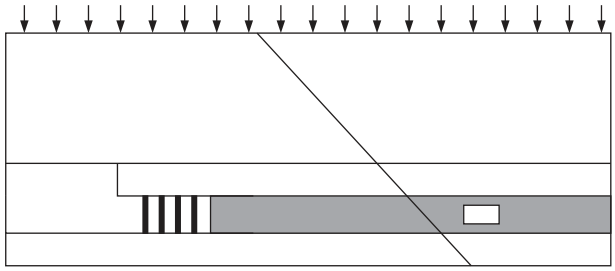

Figure 16: The numerical model of forward direction fault (the periodical fracture).

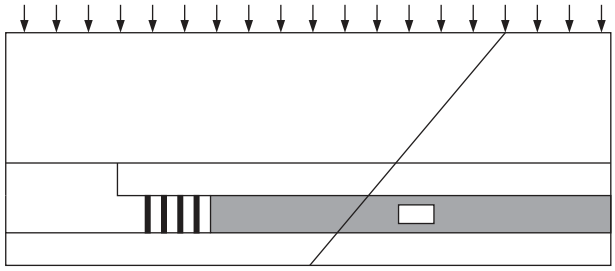

Figure 17: The numerical model of reverse direction fault (the periodical fracture).

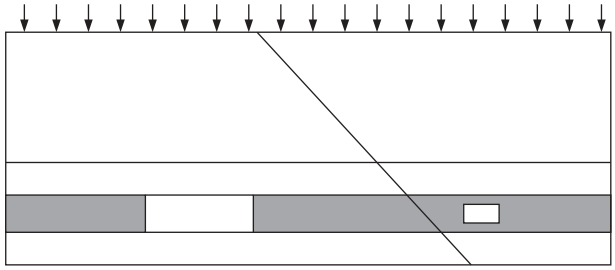

Figure 18: The numerical model of forward direction fault (the initial fracture).

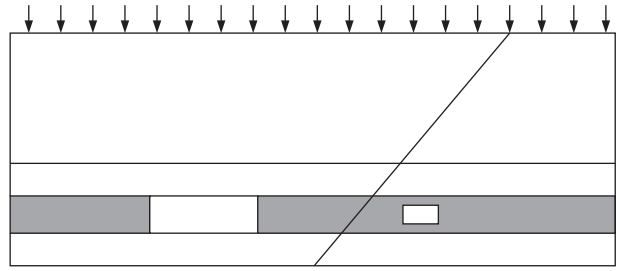

Figure 19: The numerical model of reverse direction fault (the initial fracture).

immediate roof gradually increases with the excavation of the working face. The maximum contact pressure is about 14.253 MPa when the working face is right under the fault. In the case of periodic fracture, the contact pressure of the upside is increasing as the work face is excavated. When the searching tunnel is excavated, the contact pressure of the upside roof does not decrease but increases slightly. Therefore, it can be concluded that the contact pressure cannot decrease with the excavation of the searching tunnel.

In the case of the reverse direction fault, the contact pressure of underside roof is increasing as the work face is excavated and it comes to the maximum 28.94 MPa. When the searching tunnel is excavated, the contact pressure is almost the same as before. In the situation of periodical fracture, the distribution of the underside contact pressure is nearly the same as it in the initial fracture, but the maximum is decreasing to 23.975 MPa. When the searching tunnel is excavated, the contact pressure of underside roof is not decreasing obviously but even increasing sometimes.

According to the calculation result as shown in Figure 28, for the initial fracture model of the forward direction fault, to carve a searching tunnel increases the displacement of immediate roof that above the exploitation center by 6.7%, decreasing the maximal contact pressure, about 0.192 MPa less than before, and increasing the maximal stress of the immediate roof, the maximal increment is about 4%.

As it is shown in Figure 29, for the periodical fracture of the forward direction fault, to carve out a searching tunnel increases the displacement of immediate roof by about 11.2%, and decreases the maximal contact pressure, about 0.386 MPa less than before; it does not release the maximal stress of the roof; on the contrary, the maximal stress increases; the maximal increment is nearly 11.6%.

For the forward direction fault, the development of the searching tunnel, whether the initial fracture or the periodical fracture, has an increasing effect on the displacement and stress of the roof and slightly reduces the contact stress at the fault. The influence on the periodical fracture is greater than that of the initial fracture.

For the initial fracture model of reverse direction fault, as it is shown in Figure 30, to carve out a searching tunnel, may result in increasing of the displacement of immediate roof by

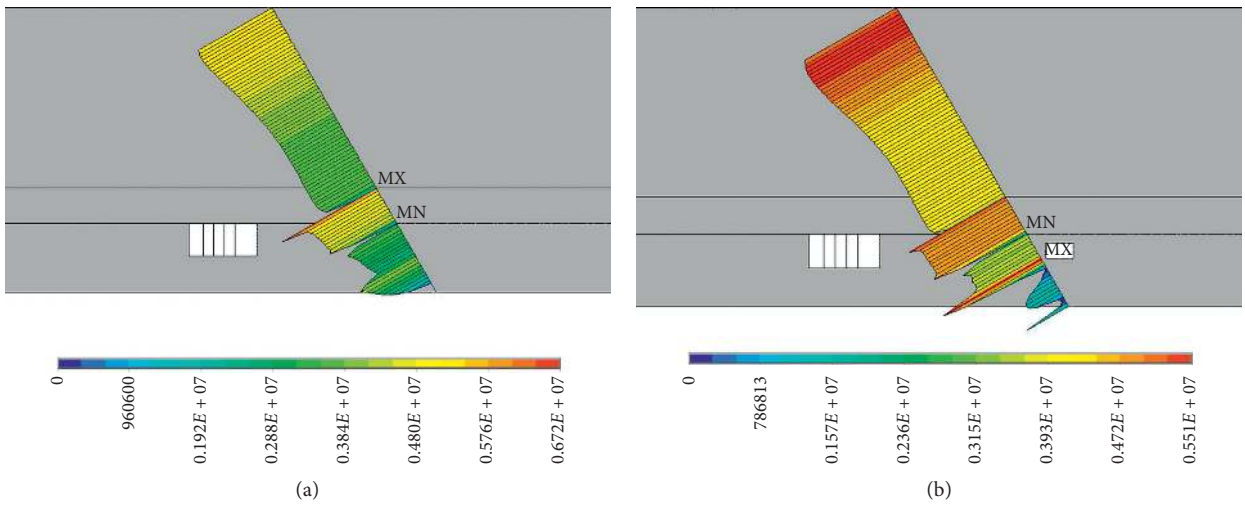

Figure 20: The nephogram of contact pressure when work face is far from the fault (forward direction fault). (a) Without searching tunnel [25, 26]. (b) With searching tunnel.

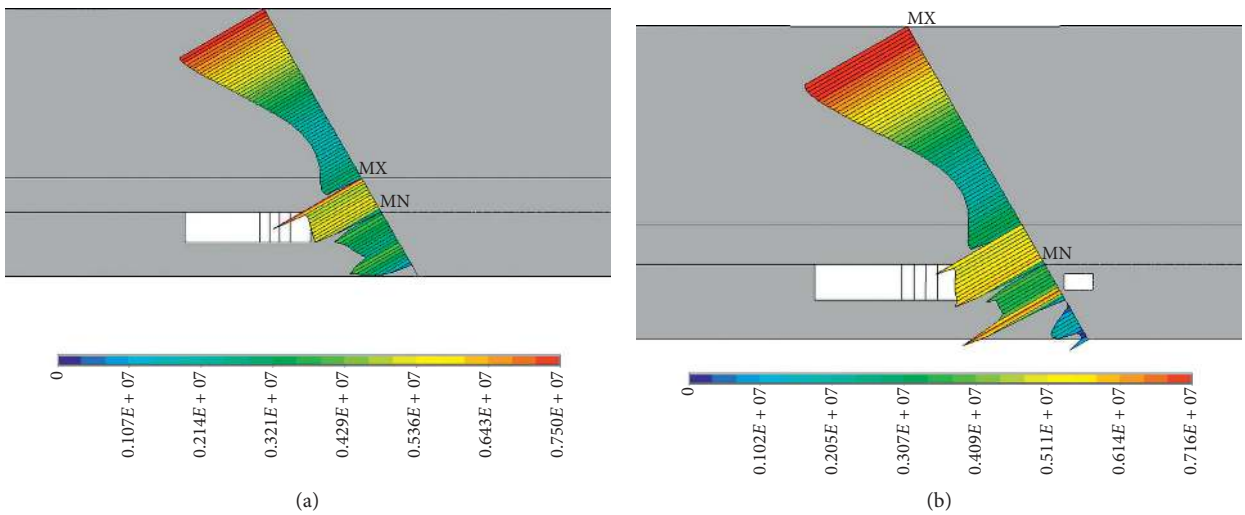

Figure 21: The nephogram of contact pressure when work face is near the fault (forward direction fault). (a) Without searching tunnel [25, 26]. (b) With searching tunnel.

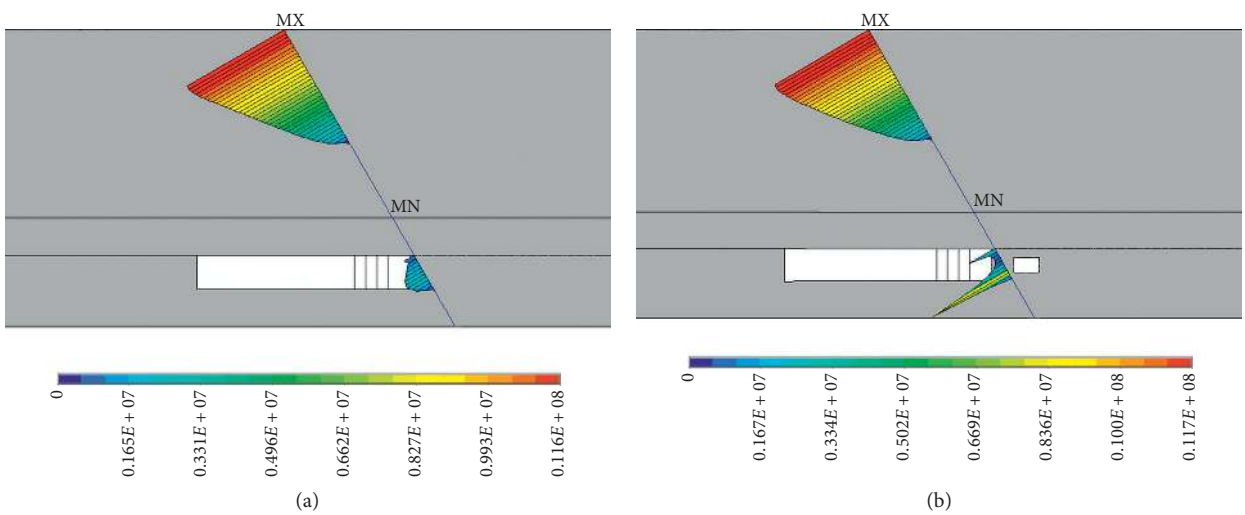

Figure 22: The nephogram of contact pressure when work face is under the fault (forward direction fault). (a) Without searching tunnel [25, 26]. (b) With searching tunnel.

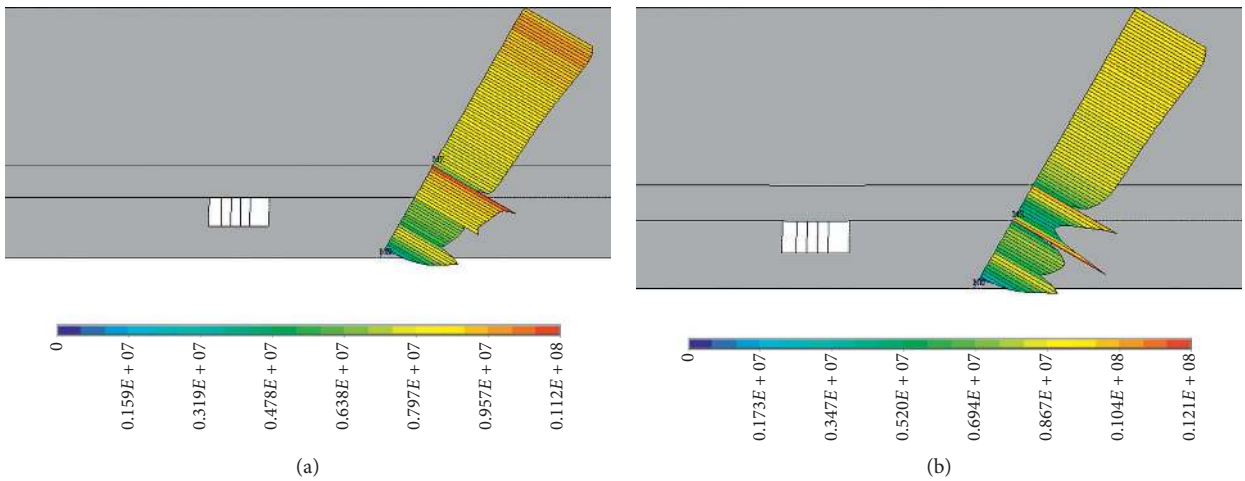

Figure 23: The nephogram of contact pressure when work face is far from the fault (reverse direction fault). (a) Without searching tunnel. (b) With searching tunnel.

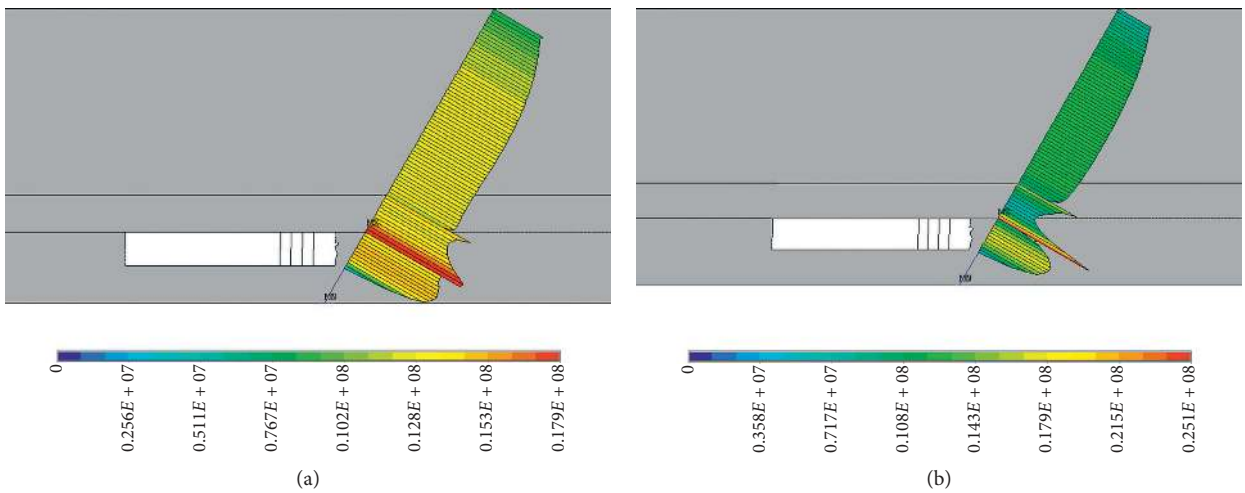

Figure 24: The nephogram of contact pressure when work face is near the fault (reverse direction fault). (a) Without searching tunnel. (b) With searching tunnel.

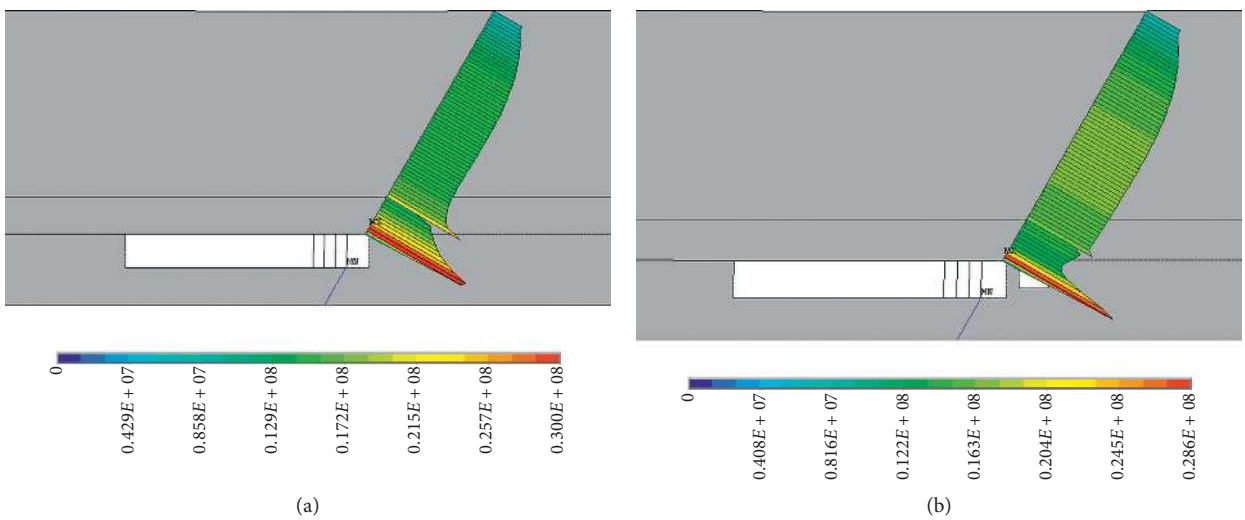

Figure 25: The nephogram of contact pressure when work face is under the fault (reverse direction fault). (a) Without searching tunnel. (b) With searching tunnel.

Table 2: The contact pressure of upside and underside of the roof.

Fracture situation	Work face	Contact pressure of forward direction fault		Contact pressure of reverse direction fault	
—	—	Upside of roof (MPa)	Underside of roof (MPa)	Upside of roof (MPa)	Underside of roof (MPa)
Without tunnel initial fracture	Far	5.116	3.019	9.893	8.317
	Near	5.044	3.629	13.471	17.895
	Under	0.000	0.000	14.253	28.939
With tunnel initial fracture	Far	4.924	3.673	9.579	8.379
	Near	4.834	4.386	13.102	18.065
	Under	0.000	0.000	14.707	28.555
Without tunnel periodical fracture	Far	6.038	3.294	10.776	9.198
	Near	6.409	4.074	11.972	14.234
	Under	4.202	0.000	13.144	23.975
With tunnel periodical fracture	Far	5.842	3.958	10.576	9.651
	Near	6.023	5.106	12.082	15.556
	Under	3.575	0.000	13.372	23.313

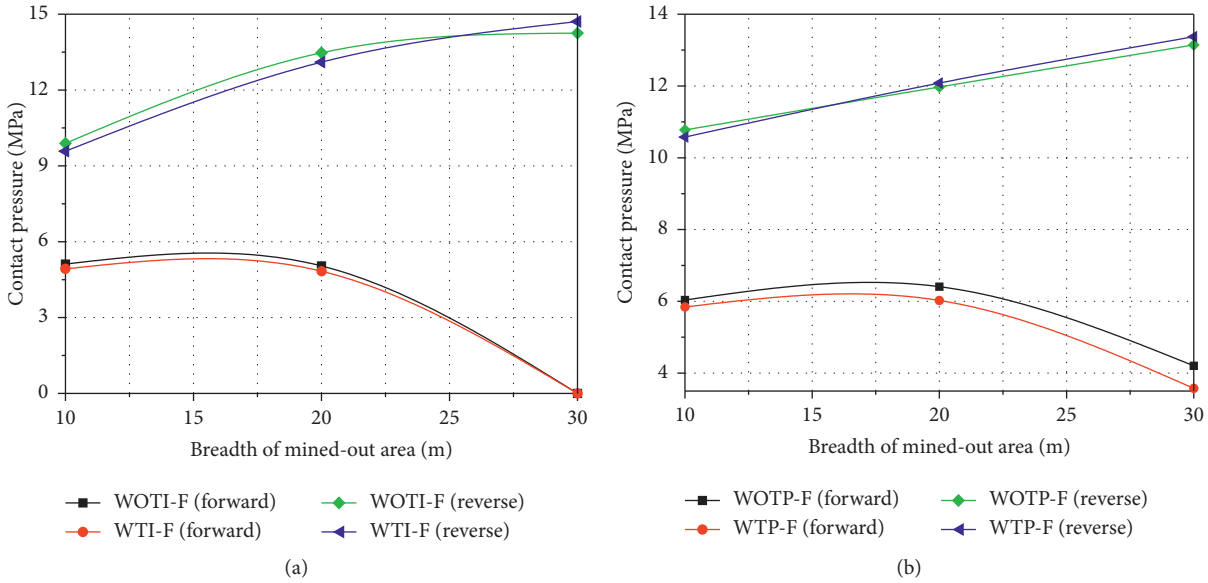

Figure 26: The change of contact pressure of upside fault along with the breadth of mined-out area (WOTI-F denotes without searching tunnel initial fracture, WTI-F denotes with searching tunnel initial fracture, WOTP-F denotes without searching tunnel periodical fracture, and WTP-F denotes with searching tunnel periodical fracture). (a) Initial fracture. (b) Periodical fracture.

2%, it decreases the maximal contact pressure about 0.384 MPa, and it also has the effect to release the maximal stress of the immediate roof nearly 25.9% at most. But to carve out a searching tunnel increases the displacement or stress of the immediate roof in forward direction fault.

As it is shown in Figure 31, for the periodical model of reverse direction fault, to carve out a searching tunnel decreases the displacement of immediate roof by 19.54%, and decrease the maximal contact pressure of fault about 0.662 MPa, it also has the effect of release the maximal stress of the immediate roof, nearly 38% at most.

For the reverse direction fault, in the case of the initial fracture, the development of the searching tunnel has almost no positive effect on the displacement of the roof and plays a role in releasing the stress of the roof. In the case of periodic fracture, the displacement and stress of the roof are greatly reduced by the excavation of the searching tunnel. The contact stress at the fault is slightly reduced when the searching tunnel is excavated.

The optimal plan is the forward direction fault without the searching tunnel or the reverse direction fault with the searching tunnel. Therefore, in the process of coal seam mining, it is not necessary to excavate the searching tunnel

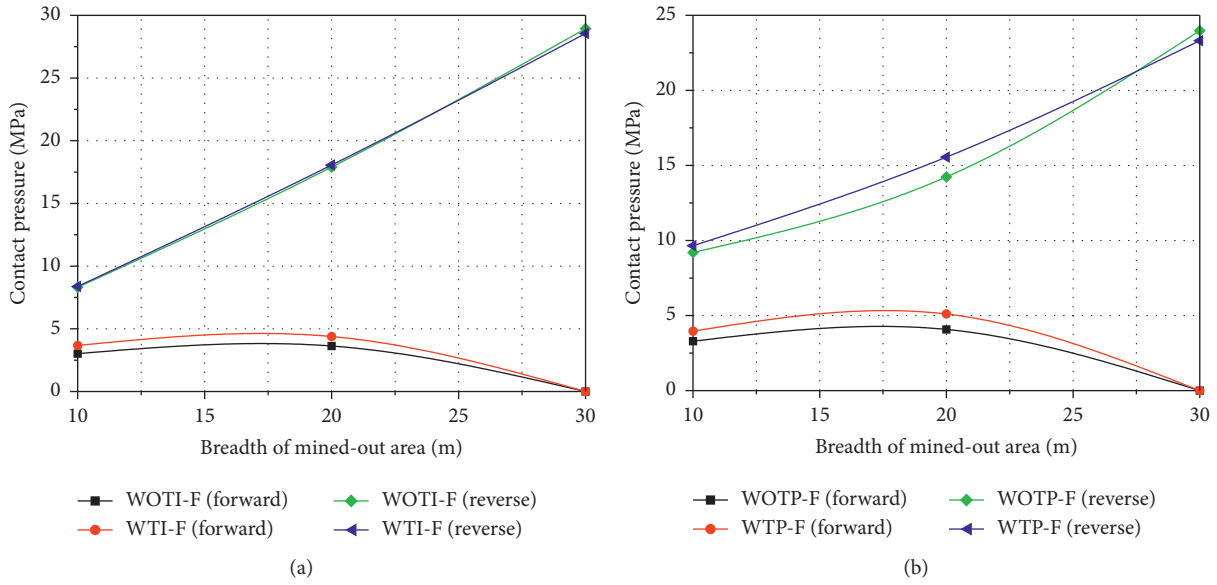

FIGURE 27: The change of contact pressure of underside fault along with the breadth of mined-out area. (a) Initial fracture. (b) Periodical fracture.

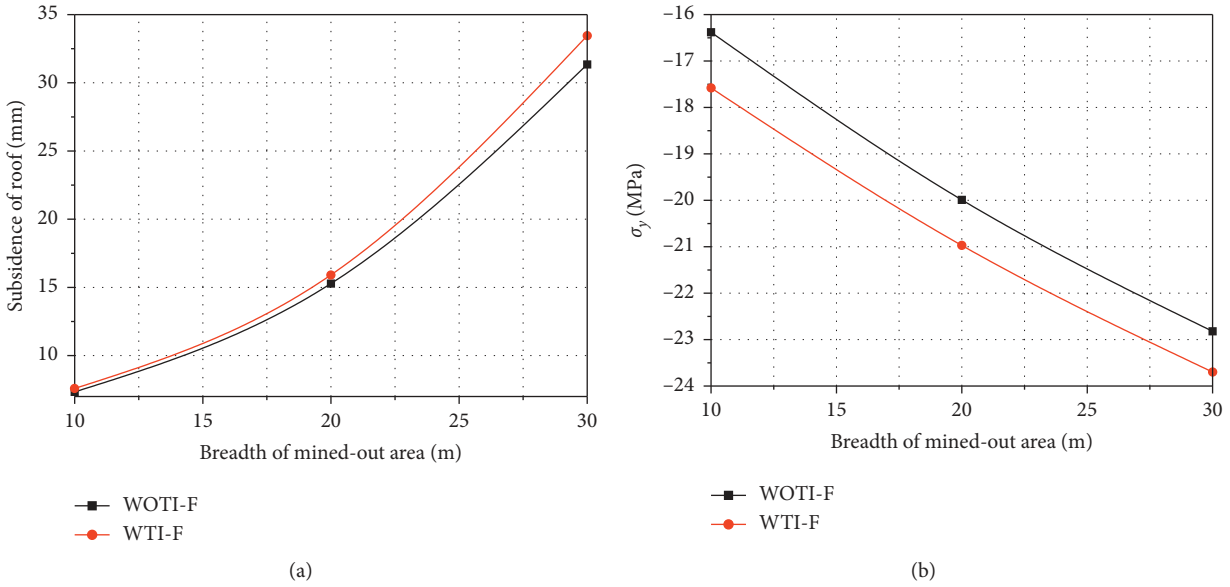

FIGURE 28: Analysis of calculation of forward direction fault with initial fracture. (a) Subsidence of the roof. (b) Vertical stress.

when the forward direction fault is encountered, and it is suggested to excavate the searching tunnel when the reverse direction fault is encountered.

Table 3 summarizes the influence of searching tunnel on the roof and fault plane. The conclusion of the searching tunnel can be obtained as follows:

(1) The contact stress at the forward and reverse direction fault is slightly reduced by the development of the searching tunnel. It can therefore be concluded that its effect to decrease the contact pressure and dissipate the energy is limited.

(2) For the forward direction fault, the displacement and stress of the roof are increased by the development of the searching tunnel, especially for the periodical fracture case. It will aggravate the fragmentation degree and make the support more difficult. Therefore, for the

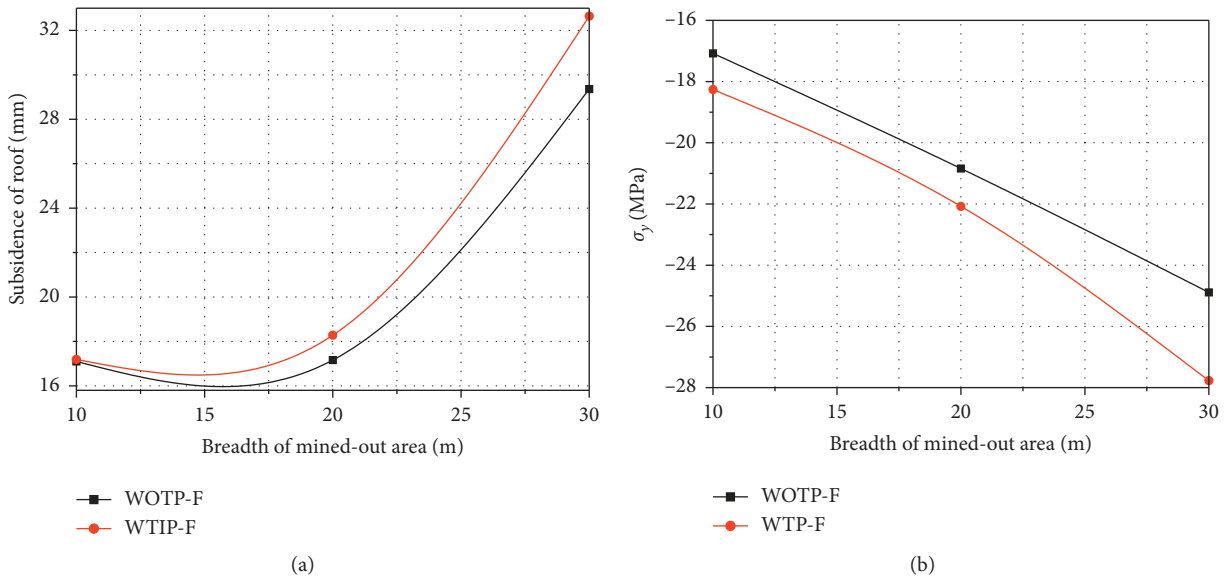

Figure 29: Analysis of calculation of forward direction fult with periodical fracture. (a) Subsidence of the roof. (b) Vertical stress.

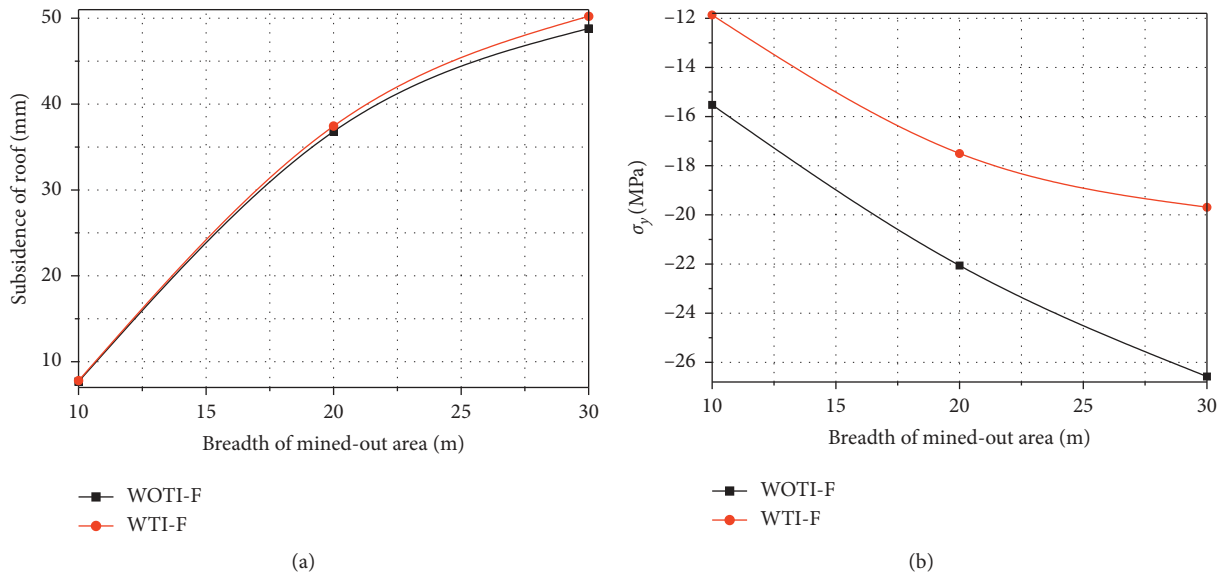

Figure 30: Analysis of calculation of reverse direction fault with initial fracture. (a) Subsidence of the roof. (b) Vertical stress.

forward direction fault, the excavation of searching tunnel can provide a better understanding of the characters of the fault, while it may not have the positive effect for the ground pressure control.

(3) Unlike forward direction fault, for the reverse direction fault, except that the displacement of the roof almost does not change in the case of the initial fracture, the displacement and stress of the roof are well released by the development of the searching tunnel. Especially during the periodic facture, the maximum stress reduction reaches 38%. Therefore, in the process of coal seam mining, it is suggested to build the searching tunnel when the reverse direction fault is encountered.

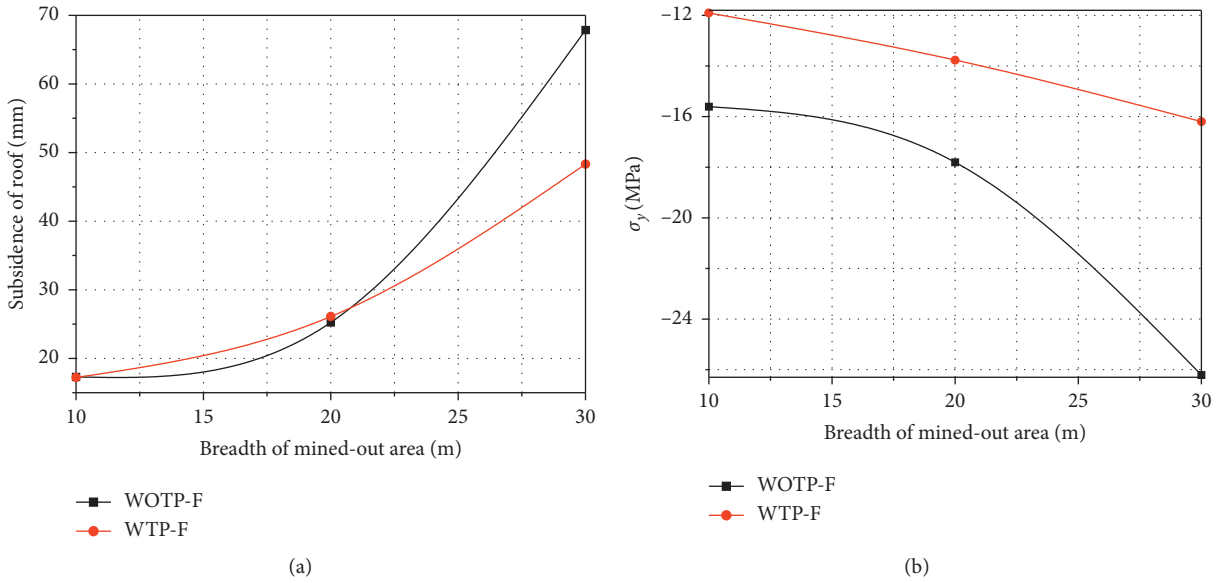

Figure 31: Analysis of calculation of reverse direction fault with periodical fracture. (a) Subsidence of the roof. (b) Vertical stress.

Table 3: Influence of searching tunnel on roof and fault plane.

Fault direction	Forward direction fault		Reverse direction fault	
Situation	Initial facture	Periodical facture	Initial facture	Periodical facture
Immediate roof displacement	+6.7%	+11.2%	+2%	−19.54%
Maximum contact stress increase of fault plane (MPa)	−0.192	−0.386	−0.384	−0.662
Maximum stress of immediate roof	+4%	+11.6%	−25.9%	−38%

4. Conclusion

In this paper, the analytical and numerical study of the work face crossing a fault is carried out. The stress distribution is investigated with the searching tunnel for both the forward direction fault and the reverse direction fault.

(1) Based on the analytical solution, the initial fracture may occur outside the support range, and the contact pressure is constant based on the beam model.

(2) For initial fracture model of forward direction fault, the displacement of the roof may increase by about 6.7%, while the maximum contact stress may have a reduction of 0.192 MPa under the effect of the searching tunnel. However, the maximum stress of the roof also does not have a good release, and the peak value may have an increase of 4%.

(3) For the periodical fracture model of forward direction fault, the development of the searching tunnel increases the displacement of the roof by about 11.2%, while the maximum contact pressure on the fault surface decreases by about 0.386 MPa. The maximum stress of the roof was also not released, which was increased by nearly 11.6% at its maximum.

(4) For the initial fracture model of reverse direction fault, to carve out a searching tunnel may lead to increasing of the displacement of roof by 2%, it decreases the maximal contact pressure about 0.384 MPa, and it also has effect to release the maximal stress of the roof, nearly 25.9% at most. But to carve out a searching tunnel may increase the displacement or stress of the roof in most time.

(5) For the periodical model of reverse direction fault, to carve out a searching tunnel decreases the displacement of the roof by 19.54% and decreases the maximal contact pressure of fault about 0.662 MPa; it also has the effect of release the maximal stress of the roof, nearly 38% at most.

(6) The optimal plan is the forward direction fault without the searching tunnel or the reverse direction fault with the searching tunnel. Therefore, in the process of coal seam mining, it is not necessary to excavate the searching tunnel when the forward direction fault is encountered, and it is suggested to excavate the searching tunnel when the reverse direction fault is encountered.

Abbreviations

q: Simplification of roof weight and overburden pressure (MPa)
h: The height of the beam section (m)

b: The width of the beam section (m)
P_1: Simplification of beam weight and overburden pressure (N/m)
P_2: Simplification of rock pressure (N/m)
F: Surrounding rock pressure (N)
a: The length of action of P_2 (m)
x: The position of the beam model section (m)
l: The length of the cantilever beam model (m)
l_1: The length of the simply supported beam model (m)
l': The length of the cantilever beam model at the fault (m)
P_3: Simplification of rock pressure at the fault (N/m)
θ: The fault dip (°)
ξ: The width of the fault in the model (m)
h (ξ): The height of the fault in the model (m)
σ_b: The stress of the beam section (N/m)
σ (x): The stress of the beam section at x (N/m)
M: Bending moment (N·m)
M (x): The bending moment of the beam section at x (N·m)
W_Z: Section modulus in bending (m^3)
E: Elastic modulus (Pa)
μ: Poisson's ratio (dimensionless).

Data Availability

The data used to support the findings of this study are available from the first author upon request.

Conflicts of Interest

The authors declare that they have no conflicts of interest.

Acknowledgments

The authors acknowledge the financial support provided by the National Natural Science Foundation of China (nos. 52078477 and 51827901) and Key Laboratory of Deep Earth Science and Engineering (Sichuan University), Ministry of Education (no. DESE202106).

References

[1] Y. Liu, "Analysis of China's coal consumption status and outlook for 2021," *Coal Economic Research*, vol. 41, no. 1, pp. 12–16, 2021.
[2] M. Qian, X. X. Miao, and F. L. He, "Analysis of key block in the structure of voussoir beam in longwall mining," *Journal of China Coal Society*, vol. 19, no. 6, pp. 557–563, 1994.
[3] J. Xu and M. Qian, "Study on the influence of key strata movement on subsidence," *Journal of China Coal Society*, vol. 25, no. 2, pp. 122–126, 2000.
[4] H. Xie, Y. Ju, M. Gao, and F. Gao, "Theories and technologies for in-situ fluidized mining of deep underground coal resources," *Journal of China Coal Society*, vol. 43, no. 5, pp. 1210–1219, 2018.
[5] X. Jiang and C. Li, "Statistical analysis on coal mine accidents in China from 2013 to 2017 and discussion on the countermeasures," *Coal Engineering*, vol. 51, no. 1, pp. 101–105, 2019.
[6] J. Yu and D. Mao, "Status and problems of roof management in China coal mines," *Coal Science and Technology*, vol. 45, no. 5, pp. 65–70, 2017.
[7] H. Zhang, D. X. Wang, and Q. F. Wang, "Analysis of the characteristic features of major severe coal mining accidents in all over the country in the period of 2005 to 2016," *Journal of Safety and Environment*, vol. 19, no. 5, pp. 1847–1852, 2019.
[8] H. Tian, Y. Zhang, H. Yan, J. Zhou, and J. Wang, "Study on safety production situation and countermeasures of coal mines in the 12th five-year period," *Safety in Coal Mines*, vol. 48, no. 10, pp. 243–245, 2017.
[9] Z. Fan, D. Mao, and Q. Qi, "Study on the warning index of roof collapse in the two-pillar-shield support working face," *Journal of Mining & Safety Engineering*, vol. 34, no. 1, pp. 91–95, 2017.
[10] J. Guo, "Influencing factors and prevention and cure process of roof mining disaster in coal seam mining," *Coal and Chemical Industry*, vol. 42, no. 6, pp. 82–85, 2019.
[11] C. Pan, B. Xia, B. Yu, P. Yu, and Y. Luo, "Novel large-scale three-dimensional fracturing experimental apparatus and application to vertical-well hydraulic fracturing of hard roof," *Geotechnical Testing Journal*, vol. 44, no. 5, Article ID 200013, 2021.
[12] Q. Huang, "Ground pressure behavior and definition of shallow seams," *Chinese Journal of Rock Mechanics and Engineering*, vol. 21, no. 8, pp. 1174–1177, 2002.
[13] X. Yan, X. Chen, and X. Yan, "Analysis on micro seismic law when fully-mechanized coalface passed through fault," *Journal of China Coal Society*, vol. 36, no. 8, pp. 83–87, 2011.
[14] P. Shi, S. Xu, and Z. Chen, "Study on strata behavior law of gob side entry driving in fully mechanized top coal caving face," *Ground Pressure and Strata Control*, vol. 1, pp. 32-33, 2004.
[15] M. Cai, P. K. Kaiser, and C. D. Martin, "Quantification of rock mass damage in underground excavations from microseismic event monitoring," *International Journal of Rock Mechanics and Mining Sciences*, vol. 38, no. 8, pp. 1135–1145, 2001.
[16] A. M. Suchowerska, J. P. Carter, and R. S. Merifield, "Horizontal stress under supercritical longwall panels," *International Journal of Rock Mechanics and Mining Sciences*, vol. 70, pp. 240–251, 2014.
[17] F. Jiang, Y. Wang, M. Ling, and Y. Yang, "Mechanism of rock burst occurring in protected coal seam induced by coal pillar of protective coal seam," *Chinese Journal of Geotechnical Engineering*, vol. 39, no. 9, pp. 1689–1696, 2017.
[18] J. Lou, F. Gao, J. Yang et al., "Characteristics of evolution of mining-induced stress field in the longwall panel: insights from physical modeling," *International Journal of Coal Science and Technology*, vol. 8, 2021.
[19] X. Hao, W. Du, Y. Zhao et al., "Dynamic tensile behaviour and crack propagation of coal under coupled static-dynamic loading," *International Journal of Mining Science and Technology*, vol. 30, no. 5, pp. 659–668, 2020.
[20] X. Hao, Y. Wei, K. Yang et al., "Anisotropy of crack initiation strength and damage strength of coal reservoirs," *Petroleum Exploration and Development*, vol. 48, no. 1, pp. 243–255, 2021.
[21] Z. Zhang, H. Xie, R. Zhang, M. Gao, T. Ai, and E. Zha, "Size and spatial fractal distributions of coal fracture networks under different mining-induced stress conditions," *International Journal of Rock Mechanics and Mining Sciences*, vol. 132, Article ID 104364, 2020.
[22] Z. Zhang, H. Xie, R. Zhang et al., "Deformation damage and energy evolution characteristics of coal at different depths,"

Rock Mechanics and Rock Engineering, vol. 52, no. 5, pp. 1491–1503, 2019.

[23] S. Hu, "TRT application of advanced water exploration technology in an iron mine roadway," *Probe-Geology and Mining Research*, vol. 1, no. 1, pp. 1-2, 2019.

[24] A. L. Nahm, "Normal fault," *Encyclopedia of Planetary Landforms*, Springer Science and Business Media, New York, NY, USA, 2014.

[25] Y. Gao, *Mechanical and Numerical Analysis of Pressure Behavior of Roof over Fault in Working Face*, China University of Mining and Technology, Xuzhou, China, 2007.

[26] X. Xu, M. Ji, F. Gao, M. Liao, and Y. Gao, "Analysis of normal fault stress and ANSYS numerical simulation based on beam model," *Metal Mine*, vol. 383, no. 5, pp. 12–14, 2008.